Self-lubricating polymer composites

Shen, Jintao

3

Fibers Filled Phenolic Composites*

In this chapter, the tribological experiments on phenol-formaldehyde composite reinforced with PTFE and glass fibers (phenolic composite liner) were performed against 100Cr6 steel and TiC/a-C:H thin film coated 100Cr6 steel. In both cases the coefficient of friction increases with increasing sliding distance until a steady-state value (≈0.116) is reached. The wear rates of the phenolic composite liner are quite close when sliding against the TiC/a-C:H coated honing ball and the uncoated ball, although a slightly lower wear rate is measured in the former case. PTFE transfer films are evident on the surfaces of the hard counterparts. The average thickness of the transfer film on TiC/a-C:H coated surfaces is about 3.8 nm. On the surface of uncoated steel honing ball, a continuous but non-uniform transfer film of around 13.9 nm average thickness was found.

This chapter has been published in the following journal:

Shen, J.T., Pei, Y.T., De Hosson, J.T.M.: Tribological behavior of TiC/a-C:H-coated and uncoated steels sliding against phenol–formaldehyde composite reinforced with PTFE and glass fibers. Tribol. Lett. 52, 123–135 (2013).

3.1 Introduction

As briefly mentioned in chapter 1, the current design of soft sliding bearings consists of a steel outer ring/plate covered with a liner of polytetrafluoroethylene (PTFE)-containing composite and an inner steel shaft. These lubrication- and maintenance-free soft sliding bearings were originally developed for outdoor applications. They are primarily used to accommodate slow rotational oscillation or reciprocating movements under heavy loads. These bearings are self-lubricating attributed to the formation of PTFE transfer films on the contact surface of the counterpart.

PTFE exhibits an ultra-low coefficient of friction, which is related to the smooth profile of rigid rod-like PTFE molecules and easy shear of PTFE lamellae. It is known that, due to the low cohesive energy of PTFE and easy sliding motion between thin slices in the band-like crystalline region, the transfer of PTFE to the surfaces of the counterparts plays an important role in the wear process. Its poor mechanical strength, excessive viscoelastic deformation and high wear rate can be modified by adding reinforcing fibers or fillers [1, 2]. The tribological performance of PTFE reinforced composites is determined by the composition and mechanical properties of the composite, and formation mechanism of PTFE transfer film [3]. Considerable work has been done on improving the tribological performance of PTFE reinforced composites sliding against steel, whilst most of them focusing on the optimization of polymer matrix and additives [1, 2, 4]. It has also been reported that the tribological performance of polymer/steel sliding couples can be further improved by surface treatment of the steel part.

During the past decades, the properties of diamond-like carbon (DLC) based coatings have been tailored by controlling their deposition process and providing promises for a wide range of tribological applications. Under unlubricated sliding against hard materials like metals or ceramics, they protect their counterparts from excessive wear by building up graphite-like layers on the surfaces of the counterparts under high contact pressure [5], and reduce stick-slip phenomenon due to their low adhesion [6].

Our previous research in MK group has made breakthroughs in the design, production and characterization of DLC-based nanocomposite coatings on various substrates, with ultra-low friction and wear rate [7-10]. Since both PTFE reinforced composite and DLC coating show self-

lubrication effects, it is tempting to investigate the tribological performance of a PTFE reinforced composite/DLC sliding couple. Up to now little work on this topic has been published. Zsidai et al. [11] found that in the case of Si doped diamond-like nanocomposite (DLN) sliding against PETP/PTFE reinforced composite at high sliding speed, the tribological behavior was mainly dominated by adhesion. Yang et al. [12] found that PTFE was transferred to the DLC surface, and roughly estimated the average transfer film thickness to be less than 1 nm after the first 10 passes by resonant nuclear reaction analysis.

In this chapter, we present a systematic study on the friction and wear behavior of PTFE reinforced composite liner sliding against steel and TiC/a-C:H nanocomposite coated steel. Tribo-tests were performed using a ball-on-disc configuration under normal load of 60 N, which simulated the situation of high-load applications of soft sliding bearings. Specially woven composite liner and optimized TiC/a-C:H nanocomposite coating were used, aiming at minimizing the wear rate of the PTFE composite liner. Wear of both the soft composite liner and the hard counterpart was evaluated by scanning electron microscopy (SEM) to understand the wear mechanism and the effect of the coating. The thickness of the transfer film was measured with an atomic force microscope (AFM). It will be shown that the results obtained contribute to the further improvement of soft sliding bearings.

3.2 Experimental

3.2.1 PTFE and glass fibers reinforced phenolic composite liner

The phenolic composite liner (PTFE filled composite liner), supplied by SKF at Nieuwegein the Netherlands, was 0.28 mm thick and consisted of phenol-formaldehyde resol resin matrix, PTFE fiber and E-glass fiber bundles that were woven into a certain pattern (N.D.A. signed). The PTFE reinforced composite is referred thereafter in the text as the ‘composite liner’. Each PTFE bundle contains around 30 filaments of diameter about 20 μm. The Young’s modulus of the composite liner is about 3-4 GPa. The liner was cured onto 5 mm thick steel backing disks (as shown in Fig. 3.1b). The content of glass fibers gradually increases from the top surface to the bottom surface (steel side) of the liner. The composite liner samples were without further cleaning for tribo-tests.

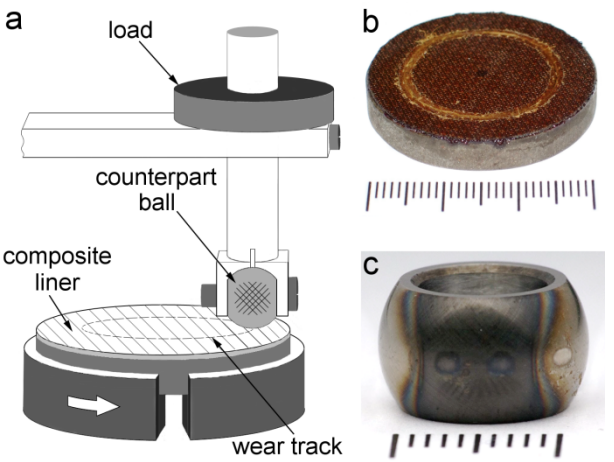

Fig. 3.1 *(a) A sketch showing the ball-on-disk configuration of tribotests with the honing pattern schematically indicated on the counterpart ball, (b) the composite liner adhered on ø30 mm steel backing disk and (c) ø13 mm 100Cr6 steel counterpart ball partly coated with TiC/a-C:H coating.*

3.2.2 Sliding counterparts

Two types of counterparts were used in the tribo-tests: ø13 mm 100Cr6 bearing steel honing balls and TiC/a-C:H nanocomposite coated 100Cr6 bearing steel honing balls (as shown in Fig. 3.1c). The surface roughness (Ra) of these steel honing balls is around 170 nm (60 μm cutoff, 705×728 μm image size), as measured with a confocal microscope. Honing pattern (grooves of near 1 μm depth with about 45° and 135° to the sliding direction as schematically indicated in Fig. 3.1a) was intentionally made by mechanical finishing on the surface of the steel honing balls. As can be seen in Fig. 2a and 2c, after being clamped into the ball holder, the angle of the grooves to the sliding direction is fixed. 100Cr6 steel has a hardness of 60-62 HRC (≈2.3 GPa) and Young's modulus 210 GPa.

TiC/a-C:H nanocomposite coating was deposited on the 100Cr6 steel honing balls, which were ultrasonically cleaned with acetone and rinsed with ethanol, and further Ar-plasma etched before deposition. The coating was deposited by reactive magnetron sputtering, the details of which are presented in Chapter 2. Properties of the nanocomposite can be found in our previous publications [8,9,13, 14]. The thickness of the coating and the intermediate layer was measured to be 1.1 μm and 0.3 μm, respectively. The surface roughness (Ra) of the honing patterned steel honing balls with

TiC/a-C:H coating is around 166 nm. The hardness and modulus of the coating are estimated to be 15 GPa and 140 GPa, respectively.

Using Dataphysics OCA-15 Goniometer, the advancing contact angles of both the 100Cr6 steel and TiC/a-C:H nanocomposite coating were measured with three liquids: water, formamide and diiodomethane. Based on the measured advancing contact angles, the surface tensions were calculated according to Owens-Wendt approach [15], the value of which is the same as surface free energy (SFE).

3.2.3 Tribological tests

Systematic study of the friction and wear behavior of the composite liner against the steel honing ball and TiC/a-C:H thin film coated honing ball was carried out using a ball-on-disk tribometer under dry sliding condition, as illustrated in Fig. 3.2a. During sliding, the ball stayed still. The normal load used was 60 N and sliding velocity was 20 mm/s. All the tests were performed at room temperature (22 ± 2°C) and a relative humidity of 35 ± 2% maintained with feedback controlled flux of dry air or water vapor into the protection box. The initial maximum Hertzian contact pressure was near 162 MPa with a contact area of 0.56 mm^2, provided that the Young's modulus of the composite liner is 3.5 GPa. The sliding distances were varied from 200 m to 1000 m. Before the tribo-tests, only the counterpart balls were cleaned with acetone and dried with clean compressed air.

After the tribo-tests, the morphology of the wear tracks of the composite liner and the wear scars of the hard counterparts were observed using optical microscopy and SEM (Philips XL-30 ESEM). Confocal microscopy (Nanofocus μSurf) was used to measure the surface profile of the wear tracks and the wear scars, for the assessment of the wear volume by a Matlab code with a margin of error of ±3% (the details of the code and calculation is seen in Appendix 1). For the calculation of the wear volume of the composite liner, only the samples without any interruption during sliding were measured, and the average values were obtained with at least two tests for each sliding distance. Energy dispersive spectroscopy (EDS) was adopted to analyze the elemental composition of the worn surfaces. The thickness of PTFE transfer films was measured using a combination of mechanical scraping and AFM (Veeco Dimension 3100) techniques. After a scratch was made with a sharp and thin razor blade, the height profiles in AFM were used to examine the thickness of the transfer films distinguished with SEM and AFM.

3.3 Results and discussion

3.3.1 Friction and wear

Typical coefficient of friction curves of the composite liner sliding against the uncoated 100Cr6 steel honing ball and the TiC/a-C:H nanocomposite film coated ball, respectively, are shown in Fig. 3.2a. The coefficient of friction increases with increasing sliding distance until a steady-state coefficient of friction is reached at around 600 m. The steady-state values of the coefficient of friction are similar (≈0.115) and low. It is clear that applying a thin TiC/a-C:H nanocomposite coating on steel honing ball, which may significantly lower the coefficient of friction in hard-to-hard contact sliding [16], has only a little effect on reducing the coefficient of friction in the case of soft sliding bearings involving PTFE. It is attributed to the excellent lubrication property of PTFE that dominates the frictional behavior of the composite liner sliding against both counterparts. A gradual increase of coefficient of friction before the steady-state is observed in both tests. This increase is attributed to the gradual increase of the contact area, due to the following two reasons: (1) viscoelastic deformation of the PTFE composite liner and (2) the gradual wear of the PTFE composite liner and the counterparts. It is noteworthy that, in the initial stage, the increase of the coefficient of friction is slower when sliding against the TiC/a-C:H coated balls. It is attributed to the self-lubrication function of the TiC/a-C:H coating itself, which may play a role before the full coverage of PTFE transfer film formed on the contact area of the coating.

As illustrated in Fig. 3.2b, the wear rates (wear volume/(load×distance)) of the composite liner show a fairly wide spread, which is due to the inhomogeneity of the fill bundles reinforced composites. When sliding against the uncoated steel honing balls, the average wear rate of the composite liner is about 2.72×10^{-14} m^3/Nm, 30 times lower than that of pure PTFE (the value measured in our tribo-test is about 6.7×10^{-13} m^3/Nm). This improvement reflects the good tribological property of the composite liner made of inexpensive and easily accessible materials. When sliding against the TiC/a-C:H coated balls, its average wear rate is slightly reduced to around 2.36×10^{-14} m^3/Nm. The average wear depth of the composite liner in the wear track of ø22 mm diameter after sliding 1000 m against the uncoated and the TiC/a-C:H coated balls are 41.8 and 36.6 μm, respectively. It is noteworthy that the increase of wear volume of the phenolic composite after the first 400 m sliding is

relatively faster than in the first 400 m, as shown in Fig. A.2 (in the Appendix 2). The accelerated wear the phenolic composite liner is detrimental to the service life of the composite liner in dry sliding bearings. Moreover, the wear rate of the phenolic composite liner lie in the medium-to-poor region and its wear volume after only 5 m (mainly plastic deformation) is as high as 2.38×10^{-10} m^3, which is probably attributed to the inhomogeneity and poor mechanical properties of the fiber bundles reinforced composites .

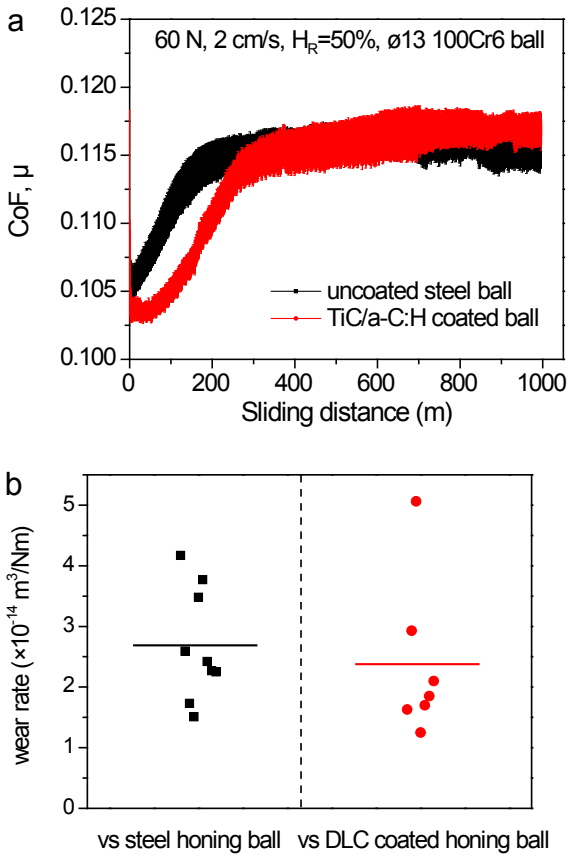

Fig. 3.2 *(a) Coefficient of friction and (b) wear volume of the composite liner sliding against ø13 mm 100Cr6 steel honing ball and TiC/a-C:H coated ball, respectively, under 60 N normal load, 20 mm/s sliding speed, 22±2 °C and 35% ±2% relative humidity.*

3.3.2 Characterization of wear morphology

Wear tracks

Figure 3.3a shows the original surface morphology of the composite liner containing PTFE and glass fiber bundles. A wear track formed after sliding 700 m against uncoated steel honing ball is shown in Fig. 3.3b, with a width of 1.38 mm. In the wear track, concentric scratches (due to the rotational sliding) and smeared PTFE fiber bundles are observed, implying heavy plough and considerable wear of the composite liner. In the wear track sliding 700 m against the TiC/a-C:H coated honing ball (Fig. 3.3c), inclined parallel lines resembling the original surface and distinguishable PTFE fiber bundles indicate less wear of the liner than the former case, in particular the phenolic resin matrix. In both cases, some micro-cracks in the resin matrix are observed in the wear track and some fractured resin lumps are also found in few locations. Such micro-cracks and fractured resin lumps cannot be found on the virgin surface of the composite liner, likely indicating the fatigue wear of the resin under repetitive sliding. It should be noted in all the tests, after the composite liner sliding against the TiC/a-C:H coated honing ball for 1000 m, the wear track morphology became alike the one shown in Fig. 3.3b. This is also an indication of the occurrence of fatigue wear in this case.

Fig. 3.4 shows the wear evolution of the PTFE fiber bundle in the wear track sliding against uncoated steel honing ball. The same location was traced at each interruption by locating the selected micro-feature marks on the surface of the composite liner to the same pixels of successive micrographs. As revealed in Fig. 3.4b, the surface of the PTFE fiber bundle was flattened after sliding for 200 m, indicating a gradual polishing of PTFE fibers. After sliding for 700 m, the PTFE fiber bundle was severely deformed and smeared, and the fibers are hardly distinguishable in Fig. 3.4c. The PTFE fiber bundle was worn off after sliding for 1000 m. Instead of the distinctive color difference shown in Fig. 3.4a-c, Fig. 3.4d was mostly filled with greenish blue color. The smeared PTFE bundle shows a similar color in the Fig. 3.4b and 3.4c, implying a high coverage of PTFE-containing third-body after sliding for 1000 m. The tracing of the wear evolution of the glass fiber bundles was also performed (not shown here). After sliding for 1000 m, some glass fiber bundles are also found to be worn off. The fragmentation and fracturing of the glass fibers were observed, which will be revealed more clearly in SEM micrographs.

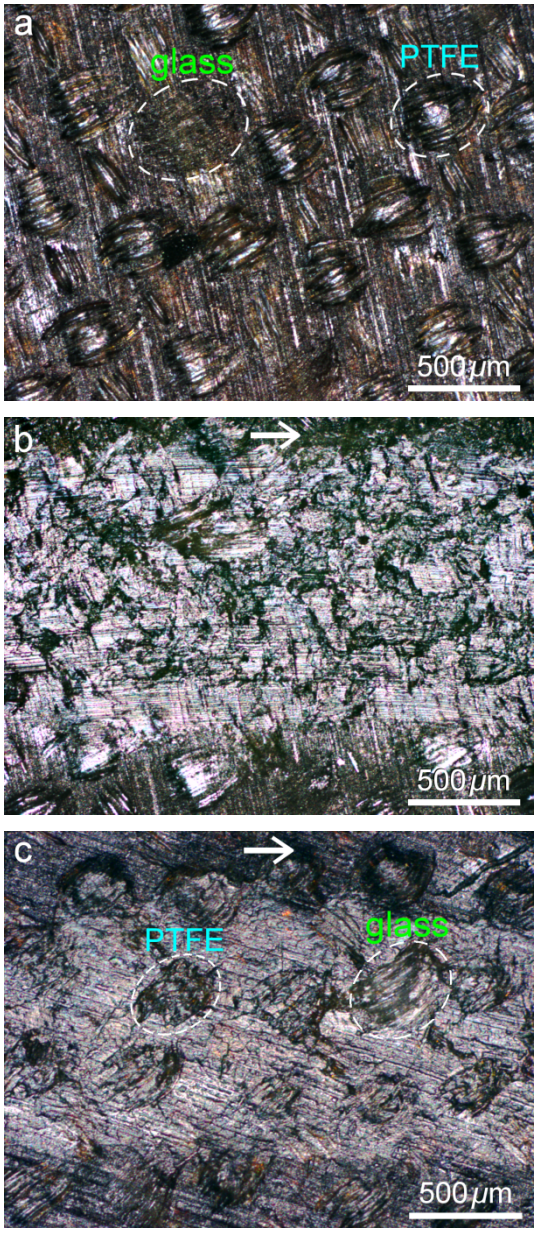

Fig. 3.3 *Optical image of the composite liner (a) and wear track (b) formed at the same location after sliding 700 m against uncoated steel honing ball; (c) wear track formed after sliding 700 m against TiC/a-C:H coated steel honing ball (under 60 N normal load and 20 mm/s sliding speed). The relative sliding direction of the still counterparts is indicated by the arrows. A PTFE fiber bundle and a glass fiber bundle are marked with dashed ellipses.*

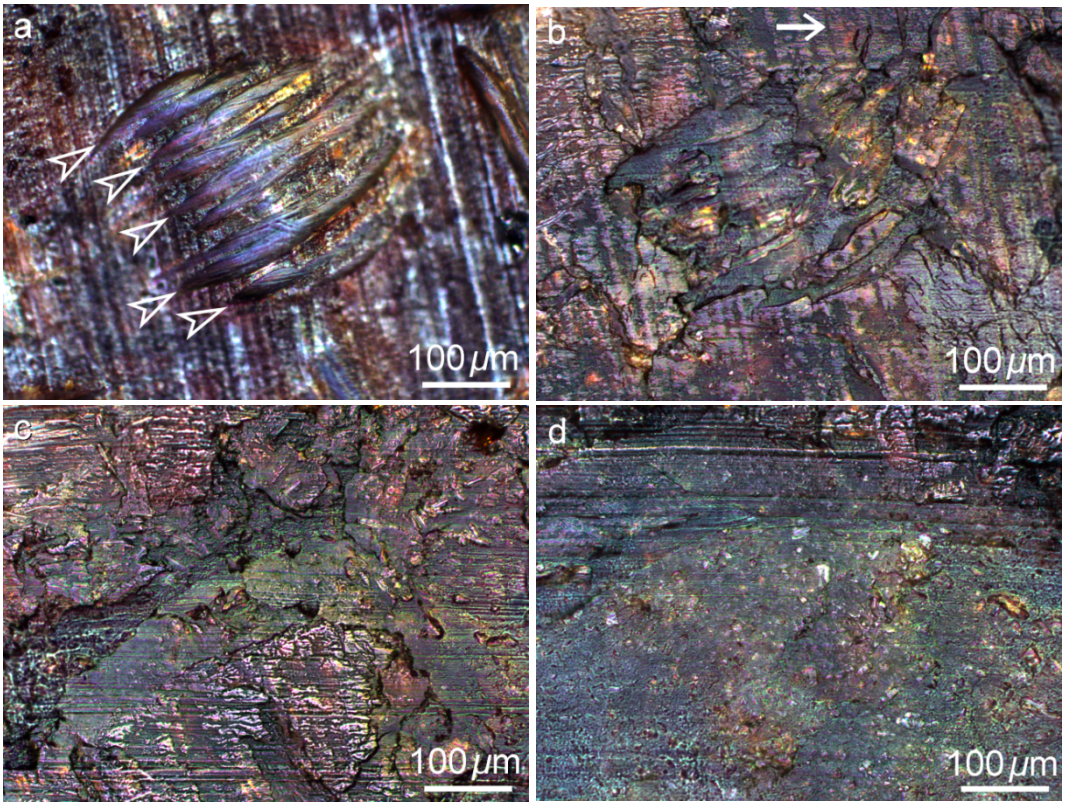

Fig. 3.4 *Optical micrographs taken at the same location revealing the wear evolution of a PTFE fiber bundle indicated with open arrows in the wear track sliding against an uncoated steel honing ball under 60 N normal load and 20 mm/s speed for sliding distance of (a) 0 m, (b) 200 m, (c) 700 m and (d) 1000 m. The relative sliding direction of the still ball is shown in (b) with an arrow, which is the same for (c) and (d).*

The worn PTFE fibers were also investigated with SEM to understand its wear process on a micro-scale. In Fig. 3.5a and Fig. 3.5c, bright dashed-line-like micro-fibrils are observed on the worn surface of the PTFE fiber, which are also found on the surface of the virgin PTFE fibers. We anticipate that the "dashed lines" around 0.2 μm wide may represent the crystalline PTFE, while the rest part may denote the amorphous PTFE. The micro-fibrils in some parts of PTFE were deformed and smeared so that they were reoriented into the sliding direction, while in other less deformed parts of a PTFE fiber the micro-fibrils still kept their direction parallel to the PTFE fiber. This sliding-induced reorientation phenomenon agrees with Makinson and Tabor's finding via electron diffraction

technique that the long PTFE molecular chains are oriented parallel to the sliding direction [17].

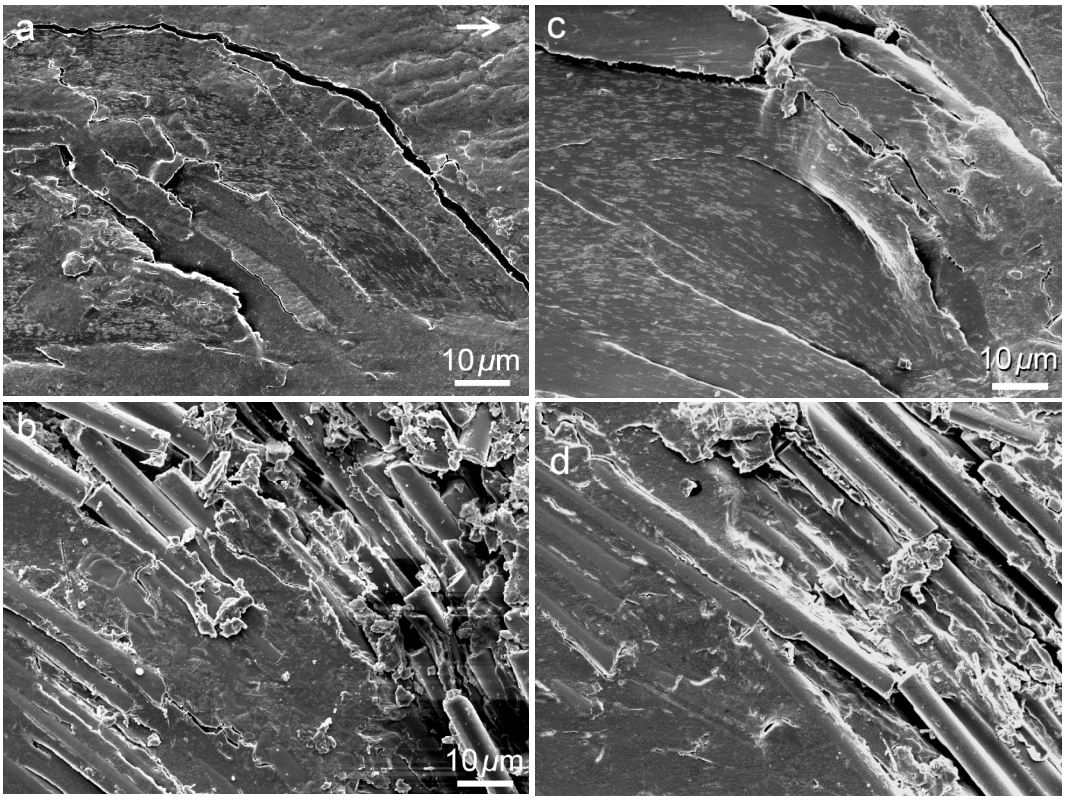

Fig. 3.5 *SEM micrographs of (a, c) worn PTFE fiber bundle containing a large amount of bright dashed-line-like micro-fibrils and (b, d) glass fiber bundle in the wear track of the composite liner, sliding for 700 m against (a, b) an uncoated steel honing ball and (c, d) an TiC/a-C:H coated honing ball under 60 N normal load and 20 mm/s sliding speed. The relative sliding direction of the balls in all 4 images is shown in (a) with an arrow.*

Although fewer glass fiber bundles than PTFE fiber bundles (around 1/20 ratio) are exposed in the wear track, they are responsible for the improved load-bearing capacity and wear resistance. When sliding against the uncoated steel and TiC/a-C:H coating counterpart, as shown in Fig. 3.5b and Fig. 3.5d, these glass fibers were de-bonded, fractured, pulled out and fragmented during the repetitive sliding under high contact stress. The main wear mechanism is considered as the fracturing and fragmentation, due to the intrinsic brittleness of the glass fibers. De-bonding and pulling out are due to the weak interfacial bonding between

glass fibers and phenolic resin matrix [18]. Most glass fibers in the wear track were covered by the third-body, while a few newly ruptured glass fibers were not covered yet, revealing the glass fibers underneath. These ruptured glass fibers were then fragmented and gradually covered by the third-body. The glass fiber fragments were collected at the interface and embedded into the softer phases or the third-body. With increasing the sliding distance, the glass fiber fragments in the third-body became shorter and some even became fine glass particles.

For a better understanding of the wear process, EDS elemental mapping was performed to reveal the mix of the soft composite components and the formation of the third body in the wear tracks. Before sliding, element F should only exist in the PTFE fiber and glass fiber bundles (E-glass fiber contains ≈1 mol.% F). At first sight of Fig. 3.6a, element F is found in almost the whole wear track sliding against the uncoated steel honing ball. The smearing of PTFE fibers, PTFE-containing third-body in the wear track and back transferring of PTFE are responsible for this result. In the close-up view of the middle part of the wear track (Fig. 3.6b) it is found that the third-body was a mixture of fractured phenolic resin, PTFE and fragmented glass fibers. In the wear track sliding against the TiC/a-C:H coated honing ball(Fig. 3.6d), bundle-like F domains and less F coverage indicate fewer third-body in the wear track and less smearing of the PTFE bundles. It is found that there was less homogeneously mixed third-body in the wear track sliding against the TiC/a-C:H coated honing ball at the same sliding distance (Fig. 3.6e). However, in both cases, fractured resin, fragmented glass fibers, and even particles are found, which reinforced the third-body and improved the wear resistance. After sliding for 1000 m, most of the wear track in both cases, especially the middle part, was covered by homogeneously mixed third-body, as a consequence of fatigue wear. Thus, the actual sliding took place between the third-body and the transfer film, which were pushed out and became wear debris during sliding.

In the composite liner, PTFE fibers contribute to the reduction of friction, while the glass fibers play a very important role in decreasing the wear rate of the composite liner. With gradually approaching the glass-fiber-rich region, their role becomes more and more prominent. Firstly, the glass fibers reinforce the composite by increasing its hardness and stiffness. Viscoelastic deformation of the PTFE and resin is also attenuated.

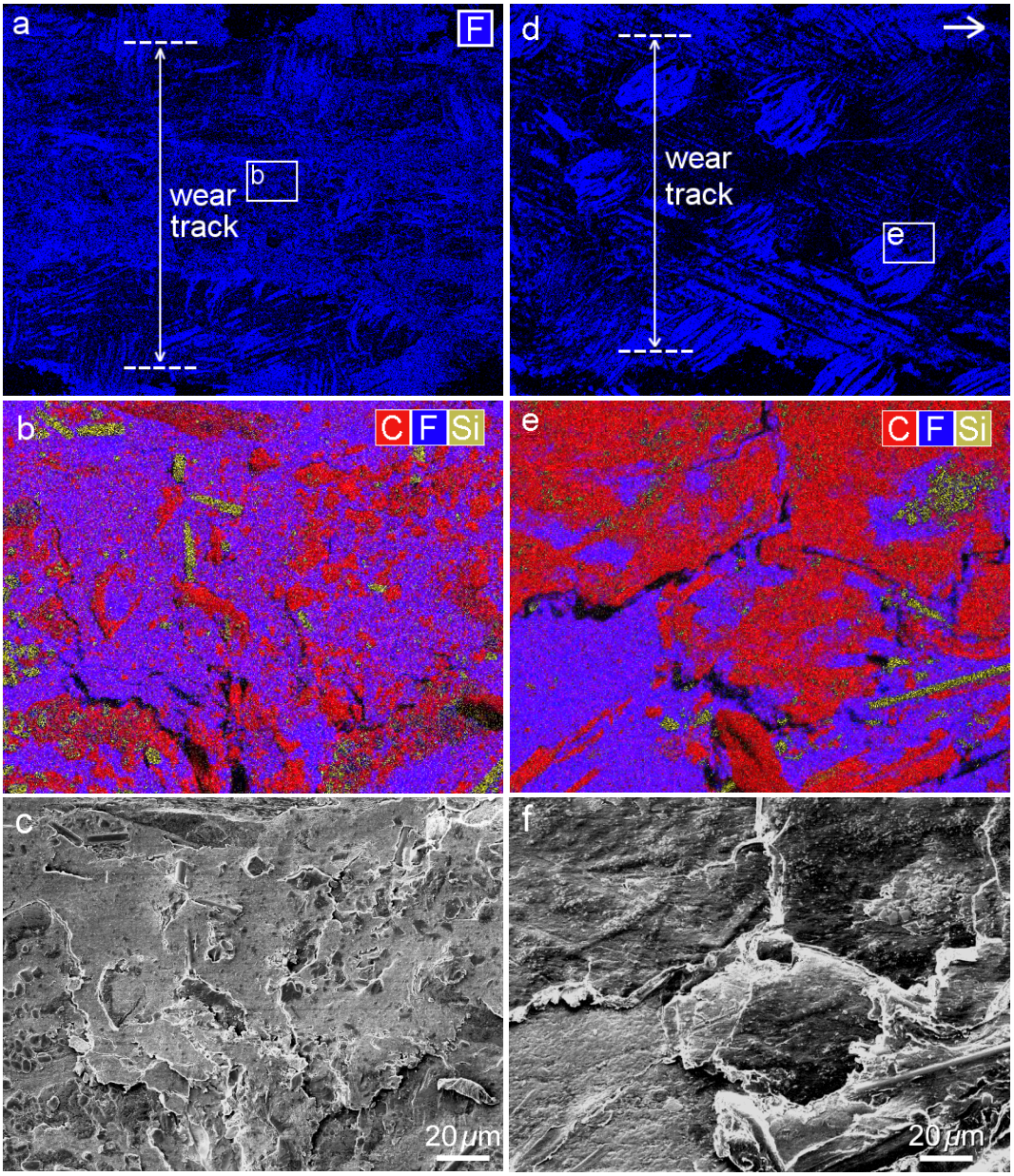

Fig. 3.6 *EDS elemental mapping: (a, d) overview of a wear track with F distribution in blue and (b, e) the middle part of the wear track of the composite liner sliding for 700 m against (a, b) the uncoated steel honing ball and (d, e) the TiC/a-C:H coated steel honing ball under 60 N normal load and 20 mm/s sliding speed. (c, f): the corresponding SEM image of (b, e).*

Secondly, although the glass fibers were initially in the form of bundles, the fractured glass fibers become more homogeneously mixed with the PTFE and resin through the formation of the third-body. The well-mixed third-body can be considered as the actual surface of the composite liner in the wear track, which contributes to a stable sliding condition and the low coefficient of friction and wear rate of the composite liner. Moreover, the abrasive glass fibers and particles are thought to increase the coefficient of friction and cause considerable wear on the counterparts, especially the relative softer steel surface (softer than the TiC/a-C:H coating). Therefore, there is a trade-off between the low coefficient of friction and the low wear rate of the composite, which requires an optimum content of the glass fibers.

According to the SEM and EDS observations, the wear mechanism of the composite liner is considered as 1) firstly the smearing and transferring of PTFE; 2) then de-bonding and fragmentation of glass fibers as well as PTFE fibers, 3) followed by cracking and fracture of resin matrix; 4) eventually generation of considerable wear debris and third-body that consists of smeared PTFE and short glass fiber fragments, fine glass particles, and fractured resin. The actual sliding mostly took place between the third-body and the transfer film after sliding for 1000 m.

Wear scars

Besides the wear tracks, detailed examination of wear scars of the hard counterparts also helps to understand the wear mechanism. As shown in Fig. 3.7, the long diameter (perpendicular to the sliding direction) of the wear scars of the uncoated and the TiC/a-C:H coated balls were measured to be around 1.4 mm and 1.2 mm, respectively, in good agreement with the width of the corresponding wear tracks. Evident wear of the uncoated steel honing ball was observed (Fig. 3.7a), with rough scratches parallel to the sliding direction. The parallel scratches, with the height of ridges up to 2 μm, were caused by the abrasion of stiff glass fibers. The rough scratches are in accordance with the concentric scratches in the corresponding wear track. On the TiC/a-C:H coated surface (Fig. 3.7b), no significant wear but slight smoothening of the surface was found. Confocal images of the wear scars were taken before and after tribo-tests as well for the calculation of the wear rate. The estimated wear rate of the steel honing ball is around 10^{-17} m^3/Nm, while that of the TiC/a-C:H coating is negligible.

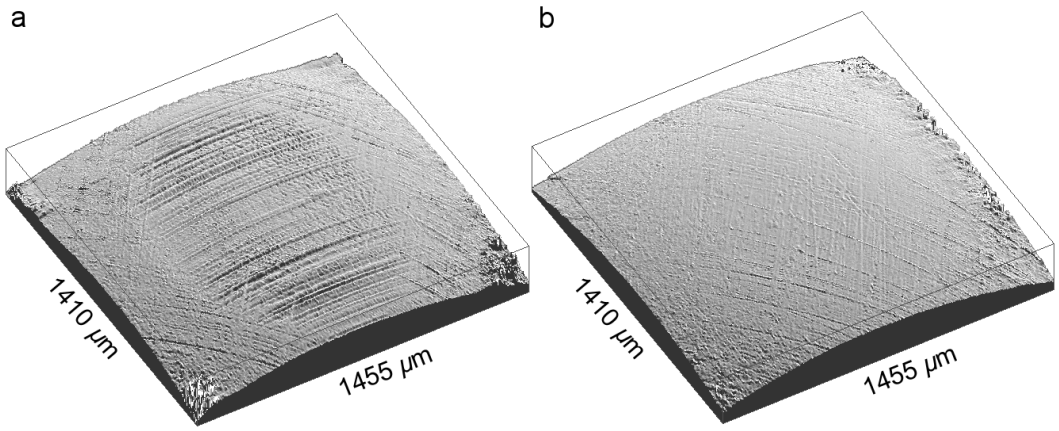

Fig. 3.7 *Confocal micrographs showing the overview of the wear scar of (a) the uncoated steel honing ball and (b) the TiC/a-C:H coated honing ball after sliding 700 m under 60 N normal load and 20 mm/s sliding speed.*

A micro-scale comparison of the hard counterparts before and after sliding against the PTFE composite liner was carried out. As shown in Fig. 3.8, the honing pattern on the steel honing ball were worn off, which occurred after sliding distance less than 200 m. Scattered polymer flakes adhering on the wear scar of the steel honing ball are observed (a typical flake is indicated by a circle in Fig. 3.8b). On the wear scar of the TiC/a-C:H coated ball, no visible polymer is found under low magnification (Fig. 3.12b), whilst a slight contrast in the flat area is observed under high magnification (Fig. 3.12c), implying that the TiC/a-C:H coating is less adhesive to PTFE and phenolic resin. Apart from few cracking and flaking-off of the coating on the edge of the grooves, slight smoothening of the coating surface and polymer films sitting in the deep grooves are observed. Although the few cracking were observed after sliding 700 m, macro-scale delamination of the coating was not observed after sliding 1000 m in any of the three tests. It is believed that the honing patterned surface of the steel substrate could alleviate the residual stress inside the coating, which improves the adhesion between the coating and the steel substrate. The highly wear-resistant TiC/a-C:H coating demonstrates its advantage over the uncoated steel honing balls. However, it is postulated that the honing pattern of the steel substrate results in the existence of many sharp edges on the TiC/a-C:H coating surface, which lead to higher abrasive wear of the composite liner and higher friction of the soft sliding bearings. It is possible that steel balls with a smoother surface as the substrate may

improve the tribo-performance of the TiC/a-C:H coated balls in soft sliding bearings, provided that the adhesion strength is high enough.

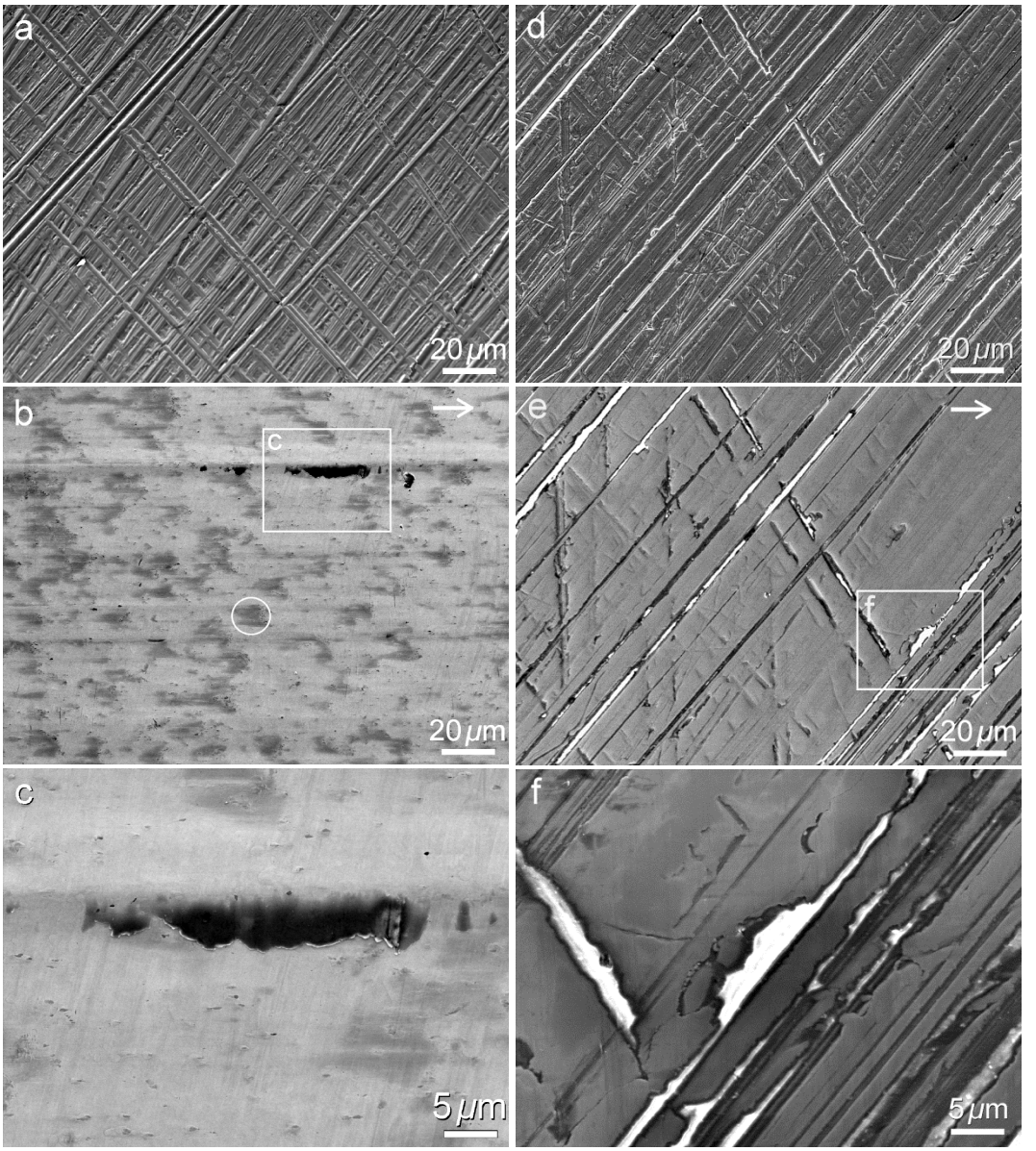

Fig. 3.8 *SEM micrographs revealing the same area on the wear scar of an uncoated steel honing ball (a) before and (b) after, on the wear scar of a TiC/a-C:H coated steel honing ball (d) before and (e) after, sliding for 700 m under 60 N and at 20 mm/s sliding speed. A polymer flake is marked in (b) by a circle. (c) and (f): the close-up view of the area indicated in (b) and (e), respectively.*

The roughness of the wear scars of the steel honing ball increases slightly upon increasing sliding distance, after a rapid drop of roughness mainly resulted from wearing off of the honing pattern (Fig. 3.9). The surface of the steel honing ball counterparts after sliding for longer than 500 m becomes rougher than that of the TiC/a-C:H coated balls. The higher roughness of the wear scar on the steel honing ball is linked to the parallel ridges, which might act as micro-knives to cut the soft composite liner (as shown in Fig. 3.7a). Therefore, the higher roughness of the wear scar of steel honing ball should be responsible for the higher wear of the composite liner.

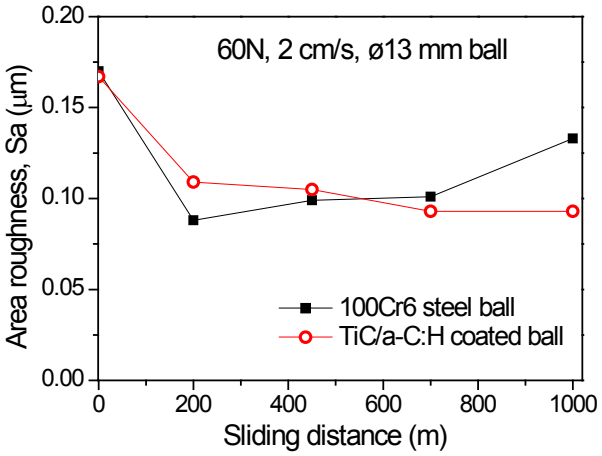

Fig. 3.9 *The roughness (cutoff length λ_c=60 µm, 705×728 µm image size) of the wear scar of uncoated steel honing ball and TiC/a-C:H coated ball, plotted against sliding distance under 60 N normal load and 20 mm/s sliding speed.*

In short, the wear rate of the steel honing balls is higher than that of the TiC/a-C:H coated balls. While rough and parallel scratches are observed in the wear scar of the former one, gradual smoothening and few coating cracking are found in the wear scar of the latter one. The harder, more abrasion resistant and less adhesive TiC/a-C:H coating on the steel surface reduces the abrasive and adhesive wear of the composite liner.

3.3.3 Transfer film

The formation of a continuous and smooth transfer film is the most crucial feature of PTFE reinforced composite liner to reduce friction in dry sliding. The elemental composition results from EDS are shown in Table 3.1. After sliding against the composite liner, the increased content of the elements C and F on the wear scar of uncoated steel honing ball suggests the

formation of transfer film on the wear scar. The increased content of element O may be associated with the existence of phenolic resin in the transfer film. As to the TiC/a-C:H coated ball, EDS measurements in the flat areas of the wear scar were carried out, to eliminate the interference of polymers accumulated in the deep grooves of the honing pattern. The signal of F was weak using 15 kV voltage, but a sharp F peak was obtained when using 1.5 kV acceleration voltage of electron beam that suits better to the K_α energy of fluorine atoms. Small amount of F and O elements found in the flat areas may imply that either the coverage of the transfer film was quite low or the transfer film was very thin considering the normal detection depth of EDS as 0.3-5 μm. The much higher F and O contents when collecting in larger area indicates that most polymers were accumulated in the deep grooves.

Table 3.1. *Elemental composition of various surfaces measured with EDS at 15 kV voltage.*

Surface	Content of elements (at.%)				
	C	F	Fe	Ti	O
as-received 100Cr6	4.6	-	88.3	-	4.4
TiC/a-C:H coating	57.9	-	1.3	32.8	2.5
wear scar of 100Cr6	6.4	12.9	69.7	-	8.7
wear scar of TiC/a-C:H	56.0	5.4	1.4	31.2	3.7
flat area on TiC/a-C:H	59.6	0.2	1.5	32.3	0.8

Further confirmation was in accordance with contact angle measurement. While the static water contact angle was measured to be 69.2° and 86.1° on the original steel and TiC/a-C:H coating surfaces, respectively, the values increased to 109.3° and 108.1° after sliding against the composite liner. The water contact angle of PTFE and phenolic resin was reported to be around 104-116° [19, 20] and 60-80° [21, 22], respectively. Therefore, it is anticipated that both wear scars were covered with transfer films that consisted mainly of PTFE, while the thick polymer flakes on the wear scar of the uncoated steel honing ball were likely phenolic resin. It is tacitly assumed that the much harder phenolic resin is less prone to be severely deformed and sheared into very thin transfer film. Some thick flakes of the phenolic resin may adhere onto the wear scar of uncoated steel honing balls, which could correspond to the dark and thick polymer flake shown in Fig. 10c. However, these thick polymer flakes can more easily be pushed out during sliding than the continuous and thin film. In contrast, no thick polymer flakes were found on the wear scar of the

TiC/a-C:H coating, consistent to the lower work of adhesion between the TiC/a-C:H coating and phenolic resin.

The thickness of the PTFE-containing transfer films on various counterparts has been reported to be within a wide range (1-1000 nm thick), due to different counterparts, experimental conditions and analysis methods. The thickness of the transfer films was measured with AFM on scratches made with a thin and flexible razor blade. As illustrated in Fig. 3.10, the scratches were evident on the wear scar, indicated by the different contrasts in the SEM micrograph (Fig. 3.10a). By comparing the contrast difference and height profile obtained from AFM (Fig. 3.10a-b), it was possible to locate the scratched areas and measure the transfer film thickness. Two very reasonable assumptions needed to be made in this method: (1) the steel and TiC/a-C:H coating were not ploughed by the razor blade, due to its comparable hardness and the gentle scratching force used; (2) the transfer films could be easily scratched away with the razor blade owing to its low hardness and the nature of van der Waals bonding between PTFE transfer film and metallic counter-faces [23].

On the wear scar of the TiC/a-C:H coated ball, a very thin and quite uniform transfer film was measured. As can be seen in Fig. 3.10b and 3.10c, the thickness of the transfer film varied in different places of the coating surface. To have a valid result, three different scratched areas were measured, with 5 profiles taken from each area. The thickness was most measured in the range of 2-6 nm as shown in Fig. A.4a (in Appendix 2) and the average value was 3.8 nm. On the wear scar of uncoated steel honing ball, the transfer film thickness was a bit difficult to measure, due to the considerably rougher worn surface itself. Therefore, more measurements were made on this sample to reach a reliable conclusion. As shown in the histogram (Fig. A.4b, in Appendix 2), the thickness of the transfer film was measured in the range of 3 to 30 nm, while a few larger values (up to ≈90 nm) were measured as well. The average value was 13.9 nm. As observed in the SEM images in Fig. 10b and 10c, the large variation in the measured thickness of PTFE-containing transfer films on uncoated steel counterparts may be related to the non-uniform distribution of the transfer film. This result is consistent with the observed polymer flakes on the wear scar of uncoated steel honing balls, while hardly any polymer flake was found on worn TiC/a-C:H coating surface (in Fig. 3.8f).

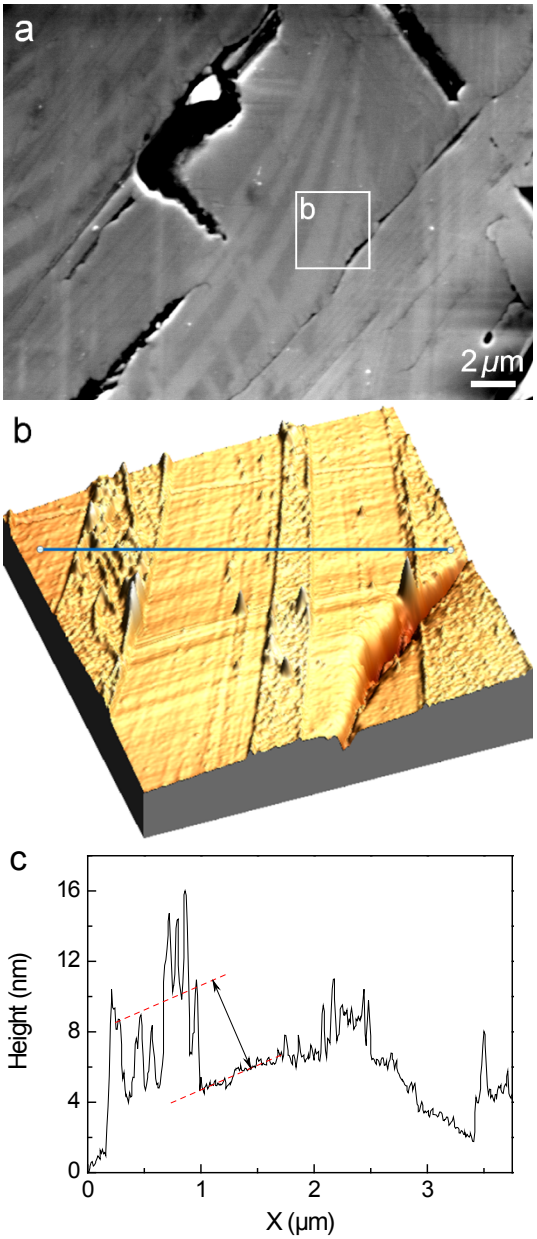

Fig. 3.10 *(a) SEM and (b) AFM micrographs of the area partly scratched with a razor blade on the wear scar of the TiC/a-C:H coated honing ball(sliding for 700 m, under 60 N normal load and 20 mm/s speed). (c) The height profile of the line marked in (b), with the average thickness of the transfer film indicated by the arrow.*

The thicker transfer film on the worn steel surface is likely associated with the stronger adhesion between the sliding couple. From the definitions of interface and surface energy, the work of adhesion (W^{adh}) between two substances can be estimated based on the following equation [21] (the derivation is in Appendix 3):

$$W^{adh} = \gamma_1^{total} + \gamma_2^{total} - \gamma_{12} = 2\sqrt{\gamma_1^d \gamma_2^d} + 2\sqrt{\gamma_1^p \gamma_2^p} \quad (1)$$

where γ_1, γ_2 and γ_{12} denote the surface free energy and interface energy of substance 1 and 2, respectively (assuming that the free surfaces are unreconstructed). *Total, d,* and *p* refer to the total surface tension, dispersive component, and polar component, respectively. The measured surface energy and the work of adhesion between the concerned solid phases are listed in Table 3.2. The surface free energy values of PTFE, phenolic resin and glass fibers are adopted from [15, 24]. As shown in Table 3.2, the work of adhesion between the steel and the resin (89.2 mJ/m^2) is significantly higher than that between the TiC/a-C:H coating and the resin (77.5 mJ/m^2). In contact to PTFE, the work of adhesion is also higher in the case of uncoated steel counterpart (57.0 mJ/m^2) than that of the TiC/a-C:H coated honing ball(52.9 mJ/m^2). A larger value of the work of adhesion indicates stronger adhesion between two solid phases [25] and more energy needed to separate the adhered phases. As a result, sliding friction increases. At the initial sliding stage when the hard counterparts are not fully covered by the transfer film, the larger coefficient of friction between the steel surface and the composite liner is partly attributed to its larger adhesive forces. The higher surface free energy of steel surface leads to the larger interfacial interaction between the steel honing ball and the PTFE composite liner. To minimize surface free energy in a contact, PTFE with lower surface free energy tends to transfer onto the counterparts of higher surface free energy [26]. When reaching the steady-state stage, the similar coefficients of friction measured in sliding against the steel honing ball and TiC/a-C:H coated honing ball are ascribed to the actual sliding between composite liner and the transfer film completely covering the wear scar of the hard counterparts. Although in some cases a larger adhesive force could give rise to a higher adhesive wear, its influence on the wear of the composite liner is not clear since a layer of transfer film covering the hard asperities on the counterparts may reduce its abrasive wear [3]. The asperity-

covering effect of the transfer film is quite complex, which is beyond the scope of this work (see also [27, 28]).

Table 3.2. *Calculated surface and interface energy, and work of adhesion between various substances based on Owens-Wendt approach.*

Surfaces	γ^{total} (mJ/m²)	γ^{d} (mJ/m²)	γ^{p} (mJ/m²)	Interfacial energy (mJ/m²)		W^{adh} (mJ/m²)	
				vs. PTFE	vs. phenolic resin	vs. PTFE	vs. phenolic resin
100Cr6 steel	58.3	33.5	24.8	20.4	8.4	57.0	89.2
TiC/a-C:H	38.2	33.5	4.7	3.8	0.008	52.9	77.5
PTFE [15]	19.1	18.6	0.5	0	4.7	38.2	53.7
phenolic resin [24]	39.3	34.5	4.8	4.7	0	53.7	78.6

3.4 Conclusions

The tribo-performance of the phenolic composite liner against the 100Cr6 steel honing ball and the TiC/a-C:H coated honing ball has been investigated. The coefficient of friction increases with increasing sliding distance until a steady-state value is reached. The wear rate of the composite liner is comparable (slightly lower) with the deposition of a thin TiC/a-C:H coating on steel surface and the steady-state coefficient of friction is also similar to that of the uncoated steel. The wear mechanism of the composite liner and the formation of transfer film are studied with optical microscopy, SEM, EDS and AFM. It can be concluded that:

(i) The wear rate of the phenolic composite liner is as high as 2.3-2.8×10^{-14} m^3/Nm, under 60N load and 20 mm/s speed. The accelerated wear and wear morphology suggests that the main wear type of the phenolic composite liner is fatigue wear.

(ii) The wear mechanism of the composite liner is a combination of smearing and transferring of PTFE, de-bonding and fragmentation of glass fibers, and cracking and fracturing of resin matrix, and generating wear debris and third-body that consists of smeared PTFE and glass fiber fragments and fractured resin. The actual sliding mostly takes place between the more homogeneously mixed third-body and PTFE-containing transfer film at the steady state.

(iii) Transfer films are found on both uncoated and TiC/a-C:H coated counterparts. The average thickness of the quite uniform transfer film is about 3.8 nm on the wear scar of the TiC/a-C:H coated ball. On the wear

scar of uncoated steel honing balls, a continuous but non-uniform transfer film of around 13.9 nm average thickness was found, due to the stronger adhesion and the existence of thick and scattered polymer flakes.

References

1. Khedkar, J., Negulescu, I., Meletis, E.I.: Sliding wear behavior of PTFE composites. Wear **252**, 361–369 (2002)
2. Bahadur, S., Tabor, D.: The wear of filled polytetrafluoroethylene. Wear **98**, 1–13 (1984)
3. Bahadur, S.: The development of transfer layers and their role in polymer tribology. Wear **245**, 92–99 (2000)
4. Lancaster, J.K.: Accelerated wear testing of PTFE composite bearing materials. Tribol. Int. **12**, 65–75 (1979)
5. Erdemir, A., Bindal, C., Fenske, G.R., Zuiker, C., Wilbur, P.: Characterization of transfer layers forming on surfaces sliding against diamond-like carbon. Surf. Coat. Tech. **86**, 692–697 (1996)
6. Yoon, E., Kong, H., Lee, K.: Tribological behavior of sliding diamond-like carbon films under various environments. Wear **217**, 262–270 (1998)
7. Pei, Y.T., Chen, C.Q., Shaha, K.P., De Hosson, J.Th.M., Bradley, J.W., Voronin, S.A., Čada, M.: Microstructural control of TiC/a-C nanocomposite coatings with pulsed magnetron sputtering. Acta Mater. **56**, 696–709 (2008)
8. Pei, Y.T., Galvan, D., De Hosson, J.Th.M.: Nanostructure and properties of TiC/a-C:H composite coatings. Acta Mater. **53**, 4505–4521 (2005)
9. Shaha, K.P., Pei, Y.T., Martinez-Martinez, D., Sanchez-Lopez, J.C., De Hosson, J.Th.M.: Effect of process parameters on mechanical and tribological performance pulsed-DC sputtered TiC/ a-C:H nanocomposite films. Surf. Coat. Tech. **205**, 2633–2642 (2010)
10. Martinez-Martinez, D., Schenkel, M., Pei, Y.T., De Hosson, J.Th.M.: Microstructural and frictional control of diamond-like carbon films deposited on acrylic rubber by plasma assisted chemical vapor deposition. Thin Solid Films **519**, 2213–2217 (2011)
11. Zsidai, L., Samyn, P., Vercammen, K., Van Acker, K., Kozma, M., Kalacska, G., De Baets, P.: Friction and thermal effects of engineering plastics sliding against steel and DLN-coated counterfaces. Tribol. Lett. **17**, 269–288 (2004)

12. Yang, E., Hirvonen, J.P.: Tribological transfer of polytetrafluoroethylene onto a diamond-like carbon film. Thin solid films **226**, 224–229 (1993)
13. Galvan, D., Pei, Y.T., De Hosson, J.Th.M.: Influence of deposition parameters on the structure and mechanical properties of nanocomposite coatings. Surf. Coat. Tech. **201**, 590–598 (2006)
14. Shaha, K.P., Pei, Y.T., Martinez-Martinez, D., Sanchez-Lopez, J.C., De Hosson, J.T.M.: Effect of process parameters on mechanical and tribological performance pulsed-DC sputtered TiC/ a-C:H nanocomposite films. Surf. Coat. Tech. **205**, 2633–2642 (2010)
15. Owens, D.K., Wendt, R.C.: Estimation of the surface free energy of polymers. J. Appl. Polym. Sci. **13**, 1741-1747 (1969)
16. Precht, W., Czyzniewski, A.: Deposition and some properties of carbide/amorphous carbon nanocomposites for tribological application. Surf. Coat. Tech. **175**, 979–983 (2003)
17. Makinson, K.R., Tabor, D.: The friction and transfer of polytetrafluoroethylene. Proc. Roy. Soc. A **281**, 49–61 (1964)
18. Al-Hashem, A.H., Tarish, H., Fallatah, G.: Cavitation erosion behavior of epoxy-, vinyl ester- and phenolic-based fiber glass composites in sea water. NACE International (2009)
19. Omenyi, S.N.: Attraction and repulsion of solid particles by solidification fronts I. Thermodynamic effects. J. Appl. Phys. **52**, 789–795 (1981)
20. Busscher, H.J., van Pelt, A.W.J., De Jong, H.P., Arends, J.: Effect of spreading pressure on surface free energy determinations by means of contact angle measurements. J. Colloid. Interf. Sci. **95**, 23–27 (1983)
21. Kaelble, D.H.: Dispersion-polar surface tension properties of organic solids. J. Adhesion. **2**, 66-81 (1970)
22. Matsushita, Y., Wada, S., Fukushima, K., Yasuda, S.: Surface characteristics of phenol–formaldehyde–lignin resin determined by contact angle measurement and inverse gas chromatography. Ind. Crop. Prod. **23**, 115–121 (2006)
23. Pepper, S.V., Buckley, D.H.: Adhesion and transfer of polytetrafluotoethylene to metals studied by Auger emission spectroscopy. NASA Technical Note (NASA TN D-6983), National Aeronautics and Space Administration, Washington D.C. (1972)

24. Lin, H.C., Kuo, S.W., Huang, C.F., Chang, F.C.: Thermal and surface properties of phenolic nanocomposites containing octaphenol polyhedral oligomeric silsesquioxane. Macromol. Rapid. Comm. **27**, 537–541 (2006)
25. Bhushan, B.: Springer handbook of nanotechnology, third ed. Springer, Columbus (2004).
26. Jain, V.K., Bahadur, S.: Material transfer in polymer-polymer sliding. Wear **46**, 177–188 (1978)
27. Wornyoh, E.Y.A., Higgs, C.F.: An asperity-based fractional coverage model for transfer films on a tribological surface. Wear **270**, 127–139 (2011)
28. Cho, M.H.: The role of transfer film and back transfer behavior on the tribological performance of polyoxymethylene in sliding. J. Mech. Sci. Technol. **23**, 2291–2298 (2010)